THE EFFECT OF RUBBER THICKNESS AND LOAD RATE ON THE INTERFACIAL FRACTURE ENERGY IN STEEL/RUBBER/COMPOSITE HYBRID STRUCTURES

E. Sarlin*, J. Vuorinen, M. Vippola, T. Lepistö
Department of Materials Science, Tampere University of Technology, Tampere, Finland
* Corresponding author (essi.sarlin@tut.fi)

Keywords: *Hybrid structure, Interfacial fracture energy, Single cantilever beam test*

1 Introduction

Hybrid structures offer a solution for a wide range of challenges faced today, since they exhibit the most advantageous properties of the constituent materials in one component. Thus, hybrids have been increasingly employed in different fields of industry [1]. Hybrid structures are mostly characterized by improved strength or stiffness combined with low weight [1], but they have potential to exhibit also other functionalities. Examples of these are good vibration damping properties [2-4], increased functional integration [5] and simpler manufacturing process [6, 7].

Organic and inorganic materials have very different physical and chemical properties. Thus the attainment of proper adhesion level between the components is one of the most challenging tasks when manufacturing polymer/metal hybrid structures [1]. Within polymer composite/steel hybrids, surface treatments, such as grit blasting, etching or anodizing, or additional surface layers, such as coupling agents or adhesives, are generally used [8, 9]. Naturally, the drawbacks of these surface treatments are increased manufacturing time and costs. To overcome some of the complexities in the manufacturing process of laminated polymer/steel hybrids, we suggest that a thin rubber layer between the steel and the composite skins could offer adequate adhesion level together with some added value, such as improved damping properties.

Rubber can be modified with additives to have good adhesion to both steel and polymers so that the joining can be done without additional surface treatments or coupling agents [10, 11]. The joining of rubber and polymer composites can be done by simultaneously vulcanizing the rubber and curing the composite [12] or by vulcanizing the rubber to an already cured composite [10]. In addition to the good adhesion and simple manufacturing process, the viscoelastic nature of rubbers improves the vibration damping properties of the hybrid structure [2, 3]. Thus, rubber is an interesting choice to be used as an adhesive in polymer/steel hybrid structures.

The most important mechanical properties of an adhesive joint are strength, stiffness, and lifetime [13]. Stiffness and strength can be studied by various test methods either in a geometry-dependent manner giving the force per unit area or length, or in a geometry-independent manner giving the energy released per unit area. In principle, the latter type of test method provides quantitative results which can be used directly in design codes and in durability models [14]. These geometry-independent test methods introduce opening (mode I), sliding (mode II), or tearing (mode III) mode of fracture of the studied interface, or a mixture of these modes. Generally, the mixed mode I+II is considered to correspond best to the realistic situations [15]. Different test method geometries, such as single cantilever beam (SCB), mixed-mode bending (MMB), double-end-notch flexure (DENF) and mixed mode flexure (MMF) introduce mixed mode I+II fracture [16, 17].

In the present study, the interfacial fracture energy of steel/rubber/composite hybrid structures was investigated by single cantilever beam test. Both rubber thickness and load rate were varied to study their effect on the interfacial fracture energy.

2 Experimental details

In this study, adhesion of a laminated glass fibre reinforced epoxy (GFRP) composite/steel hybrid was studied. As an adhesive between the steel and the GFRP layers, an EPDM based rubber was used. Two kinds of samples were studied: one where the pre-crack was located in the steel/rubber interface and another where the pre-crack was located in the composite/rubber interface.

The steel was a passivation treated cold rolled mild steel EN 10130 DC01 (Rautaruukki Oyj, Finland). The GFRP was manufactured in-house by vacuum infusion of stitched 0/90 E-glass fibre fabrics (682 g/m^2, Ahlstrom Oyj, Finland) and SR 1660 / SD 7820 epoxy (Sicomin Composites, UK). The fibre content of the composite was about 45 vol-%. The heat resistant epoxy was chosen in order to resist the vulcanizing temperature (130 °C) of the rubber. The rubber was manufactured by Kraiburg GmbH, Germany and it was particularly designed to create a strong adhesion between the steel and the GFRP layers used in this study.

Prior to rubber bonding, a HexForce® T470 (Hexcel Co., USA) peel ply was removed from the GFRP surface to be adhered and the steel surface was rinsed with ethanol and acetone to remove oil and grease residues. Other surface treatments were not used.

The steel/rubber/composite hybrid structure was manufactured by vulcanizing the rubber between the metal and the composite layers under heat and pressure (at 130°C and 1.2 MPa). Three different rubber thicknesses, namely 0.5 mm, 0.7 mm and 1.6 mm, were used. Thin metal wires between the steel and GFRP sheets ensured uniform rubber thicknesses during the vulcanization. A 30 µm thick polymer layer was used to produce a pre-crack on the composite/rubber or the steel/rubber interfaces.

The thicknesses of the rubber layers were verified from cross-sectional samples with optical stereomicroscope Leica MZ 7.5. The quality of the hybrid structures and especially their interfaces were investigated with Scanning Electron Microscope (SEM) Zeiss ULTRAplus. Conventional metallographic cross-sectional sample preparation method, including cutting the sample from the original specimens, mounting in epoxy, grinding, and polishing, was used to prepare the cross-sectional samples for SEM. Prior to SEM investigations, the SEM samples were carbon coated to ensure their conductivity under the electron beam.

Adhesion properties of the structures were studied in single cantilever beam (SCB) test geometry which introduces a combined mode I+II fracture. The 20x180 mm sized samples were extracted from larger laminates by water jet cutting. A stiffener was glued on to the steel sheets to prevent the bending of the steel during testing. Schematic picture of the test and sample geometry is shown in Fig. 1. The tests were performed using a servohydraulic mechanical testing equipment MTS 810 TestStar with a 10 kN load cell.

The tests were performed under displacement control. Three different cross head rates, namely 0.1 mm/min, 1 mm/min and 10 mm/min, were used in this study. The propagation of the delamination was observed visually with the aid of a magnifying glass and a grid painted on the both sides of the samples. At least three samples for each sample type and test conditions were tested.

The interfacial fracture energy was calculated from the load/displacement data of the servohydraulic testing machine by a compliance calibration method. The method assumes that the relationship between the crack length and compliance can be written as [18]

$$C = ma^3 + C_0 \qquad (1)$$

where a is the crack length, m is the slope of the compliance C versus the cubic of the crack length a^3 curve and C_0 is obtained from the intersection of the aforementioned curve with the vertical axis. The strain energy release rate can be calculated from Equation (2) [18]:

$$G_{I/IIC} = \frac{3P^2ma^2}{2w} \qquad (2)$$

where P is the load applied and w is the specimen width.

3 Results

The hybrid structures were first studied by optical microscopy and SEM. Fig. 2 shows cross sectional images from the sample with 1.6 mm thick rubber layer. The interfaces between steel and rubber, and composite and rubber were tight and no air bubbles or areas without proper contact were observed between the components. The quality of the interfaces was similar for the samples with thinner rubber layer.

The SCB tests were started with the samples having the pre-crack between the steel and the rubber. However, during these tests the crack always deflected to the composite/rubber interface, shown schematically in Fig. 3. Therefore, only the interfacial fracture toughness of the composite/rubber interface could be determined.

Typical load vs. displacement curves from the SCB tests of rubber/composite interface are shown in Fig. 4 for two different rubber thicknesses. The samples showed initial linear behaviour until the maximum load was achieved. The maximum load depended on rubber thickness and cross head rate (Table 1). Similar dependency has been found for thermoplastic/steel hybrids in literature [18]. Typical compliance C versus the cubic of the crack length a3 curves are shown in Fig. 5 (see also Table 2).

The 1.6 mm thick rubber layer exhibited directionally unstable cracks and crack propagation on both interfaces. Thus these samples could not be used to determine the interfacial fracture toughness. Therefore, the interfacial fracture energies were measured only for the rubber thicknesses of 0.5 mm and 0.7 mm, shown in Fig. 6. Thicker rubber led to lower interfacial fracture energy values. The cross head rate dependence was studied with rubber thickness of 0.7 mm for which the interfacial fracture energy increased with increasing cross head rate, as shown in Fig. 7.

4 Discussion

We assume that the reason for the crack deflection from the steel/rubber interface towards the composite/rubber interface is due to the higher strength of the steel/rubber interface when compared to the cohesive strength of the rubber. Thus the results of the steel/rubber interface remain at a qualitative stage for all rubber thicknesses and load rates and it can be only concluded that the steel/rubber interface is stronger than the rubber. However, this is a good result which allows the use of cohesive rubber strength instead of steel/rubber interfacial fracture toughness when simulating the hybrid structure.

The direction of the crack propagation in homogenous materials is related to the stress and energy state at the crack tip [19]. This criterion can be extended into a bi-material interface although the toughness anisotropy in the vicinity of the interface has an additional effect on the crack path direction [19, 20]. If there is an adhesive at the interface as a third component, the adhesive thickness also has its effect on the crack direction [19]. Our tests showed, that the samples having the pre-crack at the composite/rubber interface, had a stable crack growth direction if the rubber layer was thin (0.5 or 0.7 mm) or unstable if the rubber layer was thick (1.6 mm). This could be explained by the combined effect of the increased adhesive (rubber) thickness and different stress and energy states at the crack tip.

The average interfacial fracture energies for different sample types are shown in Table 3. The values are moderate when compared to corresponding values obtained for glass fibre reinforced epoxy/nickel-titanium interface (~2100 J/m^2 [21]) or for glass fibre reinforced thermoplastic/steel interface (850-1300 J/m^2 [18]).

Generally, excessively thick adhesives result in poor strength [22]. The expected increase in the interfacial fracture energy with decreasing rubber thickness was observed also in our tests (Fig. 6 and Table 3). Thus, when aiming to high interfacial strength, a thin rubber layer is preferred. However, the thinner the rubber layer, the smaller is its effect on the damping properties of the hybrid structure [3]. Therefore, the final thickness of the rubber layer has to be optimized between the acquired adhesion strength and damping properties of the hybrid structure.

The load rate dependence of interfacial fracture energy has been studied in various studies. In the review paper of Cantwell and Blyton [23], it is concluded that for mode I fracture brittle-matrix (epoxy) composites as well as for neat resins, the G_{Ic} is either insensitive to or shows a slight increase with increasing loading rate. In contrast, rubber modified epoxy composites and neat resins show a reduction in G_{IC} with increasing loading rate [23]. For mode II fracture, the different studies reviewed in [23] show contradictory results, but the writers expect an increase in interlaminar fracture with increasing loading rate bot for tough and brittle-matrix composites.

The strain rate dependence of the interlaminar fracture energy in bi-material systems have been studied mainly by thermoplastic/metal systems. Examples of these are the studies of Reyes and Gupta [18], Cortés and Cantwell [24] and Reyes Villanueva *et al.* [25] who have studied the strain rate dependence of the interlaminar fracture energy with the SCB test geometry. In these studies, a clear increase in the interfacial fracture energy with increasing loading rate [18, 25] or only a minor effect [24] was found for different thermoplastic/metal systems. Our thermoset/steel samples showed an intermediate behaviour when compared to these studies.

Although the results of the current study could refer to a linear effect of load rate on the interfacial fracture energy, more load rates should be studied to validate this conclusion. For thermoplastic/aluminium interface, a linear behaviour has been observed in the load rate range 0.1-100 mm/min, beyond which the behaviour was non-linear [25].

5 Conclusions

In this study, the effect of rubber thickness and load rate on the mode I+II interfacial fracture energy in steel/rubber/composite hybrid structures was investigated. The interfacial strength of steel/rubber joint was observed to be higher than the cohesive strength of rubber. For the composite/rubber interface, it was observed that the interfacial fracture toughness increases with increasing load rate and decreasing rubber thickness. These results are in agreement with findings presented in the literature for composite materials. Thus the introduction of rubber into a hybrid structure does not alter the behaviour of the structure radically and the assumptions made about the behaviour of conventional sandwich and composite structures can be applied for these steel/rubber/composite hybrids as well. Even though the present study showed moderate interfacial fracture energy values when compared to the corresponding values obtained for thermoplastic/steel interface, the structure is still a promising choice for such real life applications as impact loaded stressed-skin constructions.

Acknowledgements

The work was funded by the Doctoral Programme of Tampere University of Technology's President. The authors acknowledge Rautaruukki Oyj for the cold rolled steel sheets and Kraiburg GmbH for the rubbers. Kosti Rämö is thanked for the manufacturing of the GFRP composites and hybrid structures used in this work

References

[1] S. T. Amancio-Filho, J. F. dos Santos "Joining of polymers and polymer-metal hybrid structures: Recent developments and trends". *Polymer*

Engineering and Science, Vol. 49, pp. 1461-1476, 2009.

[2] J. M. Kelly, D. Konstantinidis ”*Mechanics of Rubber Bearings for Seismic and Vibration Isolation*”. Wiley, 2011.

[3] E. Sarlin, Y. Liu, M. Vippola, M. Zogg, P. Ermanni, J. Vuorinen, T. Lepistö ”Vibration damping properties of steel/rubber/composite hybrid structures”. *Composite Structures*, Vol. 94, pp. 3327-3335, 2012.

[4] G. L. Ghiringhelli, M. Terraneo, E. Vigoni ”Improvement of structures vibroacoustics by widespread embodiment of viscoelastic materials”. *Aerospace Science and Technology*, http://dx.doi.org/10.1016/j.ast.2012.11.003, 2012.

[5] O. J. Zoellner, J. A. Evans “Plastic-metal hybrid: A new development in the injection molding technology”. *Proceedings of SPE Annual Technical Conference (ANTEC)*, San Francisco, CA, USA, pp. 1-4, 2002.

[6] E. Sarlin, E. Heinonen, J. Vuorinen, M. Vippola, T. Lepistö ” Adhesion properties of novel corrosion resistant hybrid structures”. Submitted to *International Journal of adhesion and Adhesives*, 2013.

[7] M. Grujicic, V. Sellappan, M. A. Omar, N. Seyr, A. Obieglo, M. Erdmann, J. Holzleitner “An overview of the polymer-to-metal direct-adhesion hybrid technologies for load-bearing automotive components”. *Journal of Materials Processing Technology*, 197, pp. 363-373, 2008.

[8] R. G. J. van Rooijen, J. Sinke, S. van de Zwaag ”Improving the adhesion of thin stainless steel sheets for fibre metal laminate (FML) applications”. *Journal of Adhesion Science and Technology*, Vol. 19, No. 16, pp. 1387-1396, 2005.

[9] J. Cognard “Some recent progress in adhesion technology and science”. *C.R. Chemie*, Vol. 9, pp 13-24, 2006.

[10] B. Crowther (Edit.) “*The Handbook of Rubber Bonding*”. Rapra Press, 2003.

[11] F. Plenk, J. Schaube “Rubberize your composites – Simple integration of new features in fiber reinforced plastics (FRP)”. *Proceedings of SAMPE Europe 30th International Jubilee Conference*, Paris, France, 2009.

[12] United States Patent 2668789 “*Composite rubber and resinous plastic materials and method of making same*”, E. H. Phreaner, 1954.

[13] A. Baldan “Review: Adhesively-bonded joints in metallic alloys, polymers and composite materials: Mechanical and environmental durability performance”. *Journal of Materials Science*, Vol. 39, pp. 4729-4797, 2004.

[14] K. L. Mittal (Edit.) “*Adhesion measurement of films and coatings, Volume 2*”. VSP BV, 2001.

[15] M. Kenane, M. L. Benzeggagh “Mixed-mode delamination fracture toughness of unidirectional glass/epoxy composites under fatigue loading”. *Composites Science and Technology*, Vol. 57, No. 5, pp. 597-605, 1997.

[16] A. J. Brunner, B. R. K. Blackman, P. Davies “A status report on delamination resistance testing of polymer-matrix composites”. *Engineering Fracture Mechanics*, Vol. 75, pp. 2779- 2794, 2008.

[17] A. Szekrényes “Overview on the experimental investigations of the fracture toughness in composite materials”. *Hungarian Electronic Journal of Science*, Mechanical section MET-020507-A , [WWW] [20.3.2013] Available in http://hej.sze.hu/

[18] G. Reyes, S. Gupta “Manufacturing and mechanical properties of thermoplastic hybrid laminates based on DP500 steel”. *Composites Part A*, Vol. 40, pp. 176-183, 2009.

[19] B. Chen, D. A. Dillard “Numerical analysis of directionally unstable crack propagation in adhesively bonded joints”. *International Journal of Solids and Structures*, Vol. 38, pp. 6907-6924, 2001.

[20] M. T. Tilbrook, K. Rozenburg, E. D. Steffler, L. Rutgers, M. Hoffman “Crack propagation paths in layered, graded composites”. *Composites Part B*, Vol. 37, pp. 490-498, 2006.

[21] P. Cortes, W. J. Cantwell, K. S. C. Kuang “The fracture properties of a smart fiber metal laminate”. *Polymer Composites*, Vol. 28, Is. 4, pp. 534-544, 2007.

[22] D. E. Packham “*Handbook of Adhesion*”. 2nd edition, John Wiley & Sons, 2005.

[23] W. Cantwell, M. Blyton “Influence of loading rate on the interlaminar fracture properties of high performance composites – A review”. *Applied Mechanics Reviews*, Vol. 52, No. 6, pp. 199-212, 1999.

[24] P. Cortés, W. J. Cantwell “Interfacial fracture properties of carbon fiber reinforces PEEK/titanium fiber-metal laminates”. *Journal of Materials Science Letters*, Vol 21, pp. 1819-1823, 2002.

[25] G. Reyes Villanueva, W. J. Cantwell, J. Cruz M., F. A. Velasco A. "The impact properties of novel thermoplastic-based fibre-metal laminates". *Proceedings of VI International Conference on Composite Materials*, Morelia, Mexico, 2003.

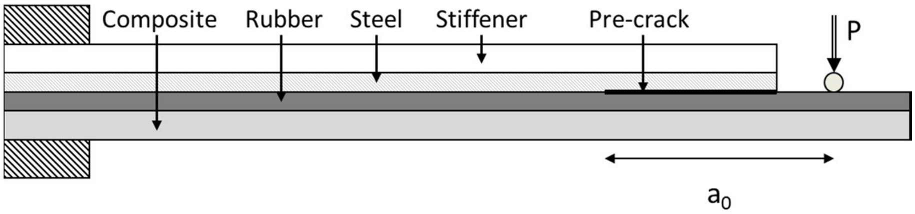

Fig. 1. A schematic picture of the single cantilever beam test and sample geometry.

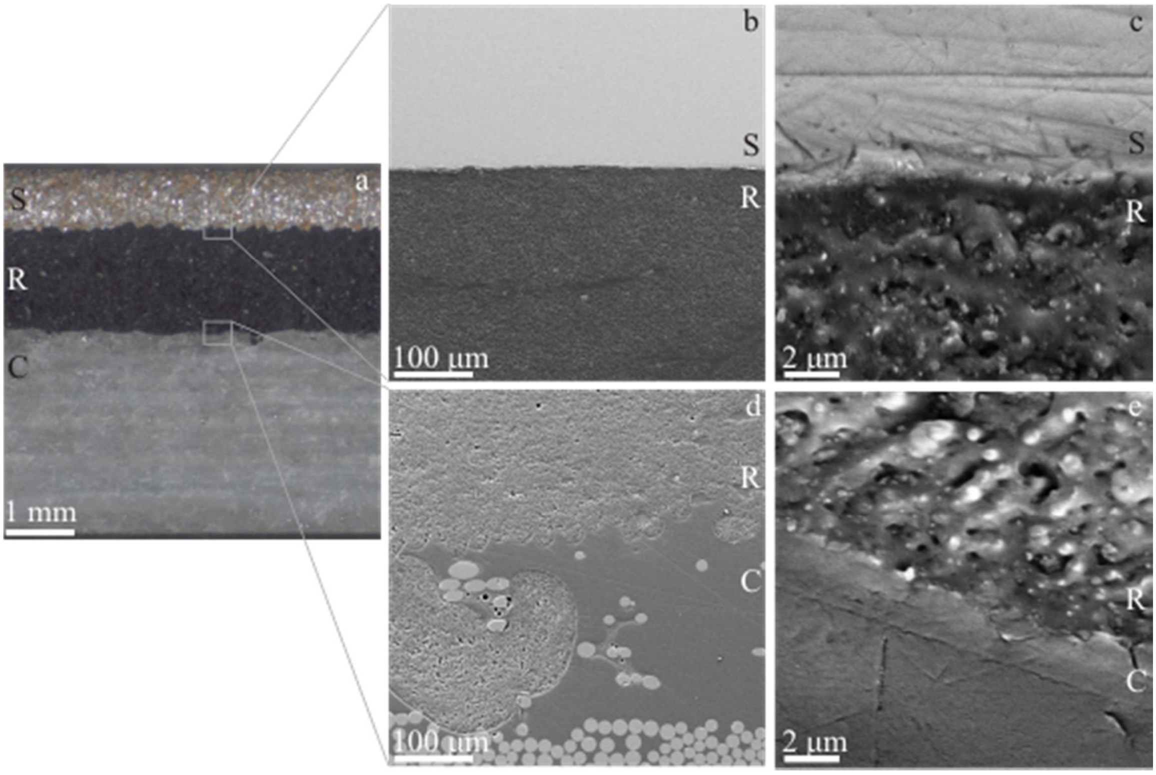

Fig. 2. a) Optical cross sectional images of the steel/rubber/composite structure and close-up SEM images b-c) from the steel (S)/rubber (R) interface and d-e) from the composite (C)/rubber (R) interface.

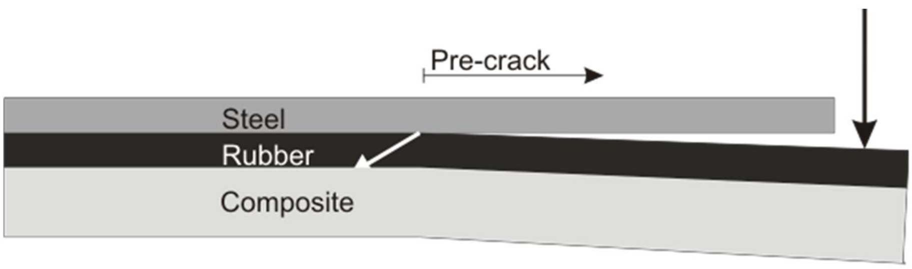

Fig. 3. A schematic presentation of the crack path at the steel/rubber interface. The white arrow in the rubber layer shows the crack path direction.

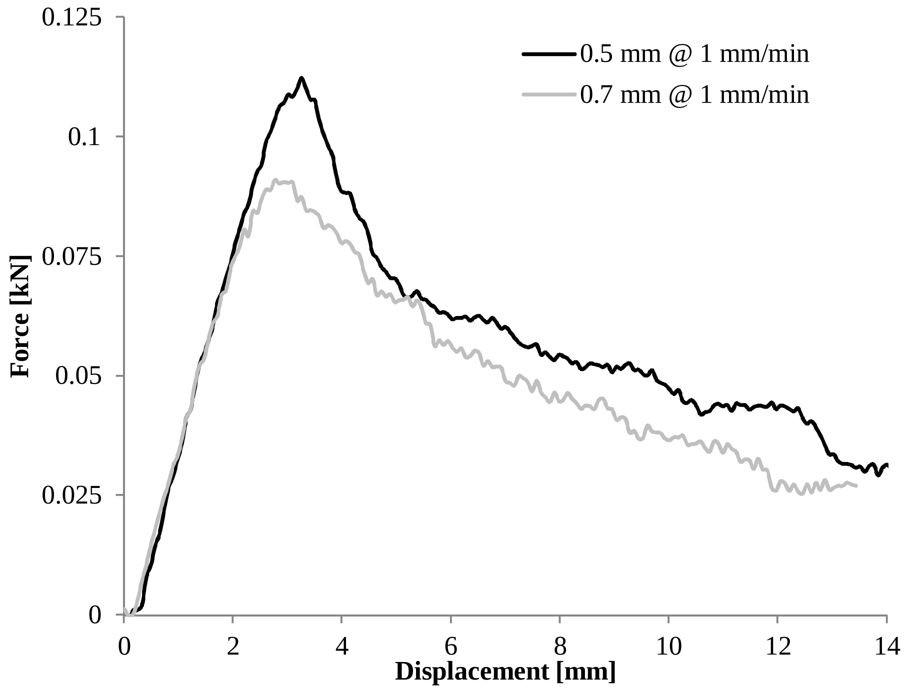

Fig. 4. Typical load vs. displacement curves from the SCB tests of rubber/composite interface for two different rubber thicknesses.

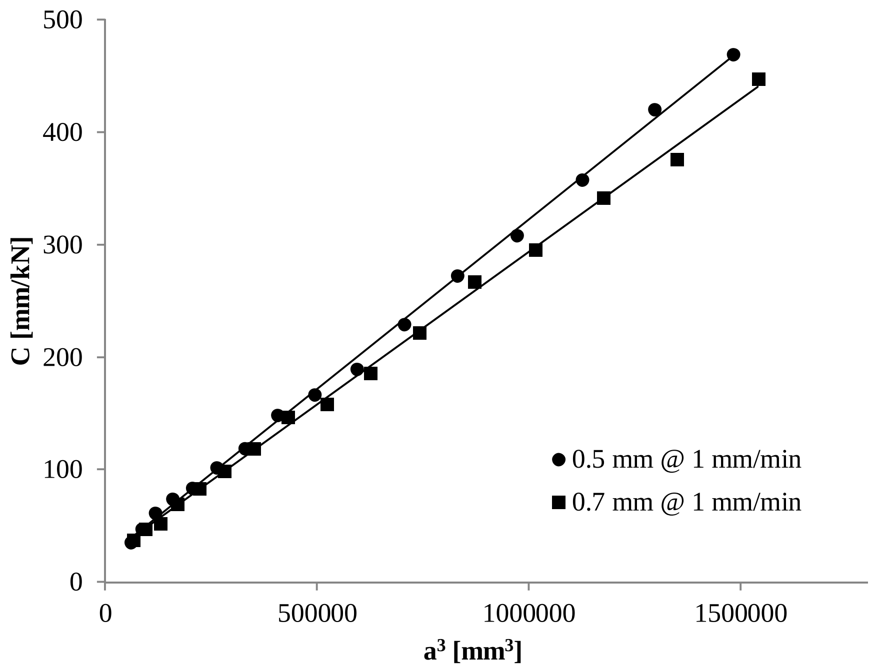

Fig. 5. Typical compliance C versus the cubic of the crack length a^3 curves from the SCB tests of rubber/composite interface for different rubber thicknesses.

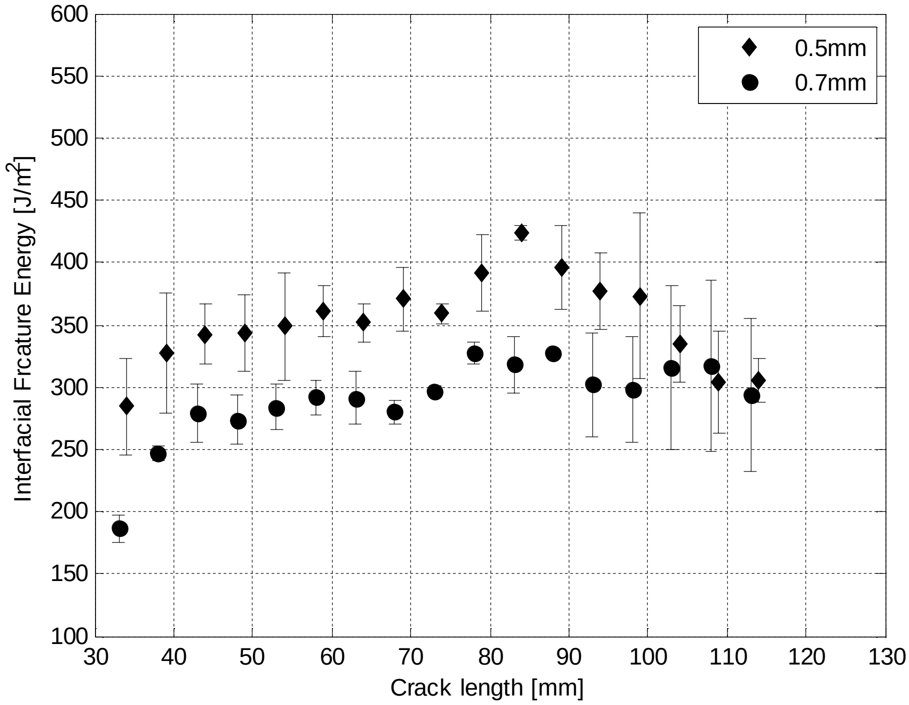

Fig. 6. The interfacial fracture energy of composite/rubber interface for two different rubber thicknesses.

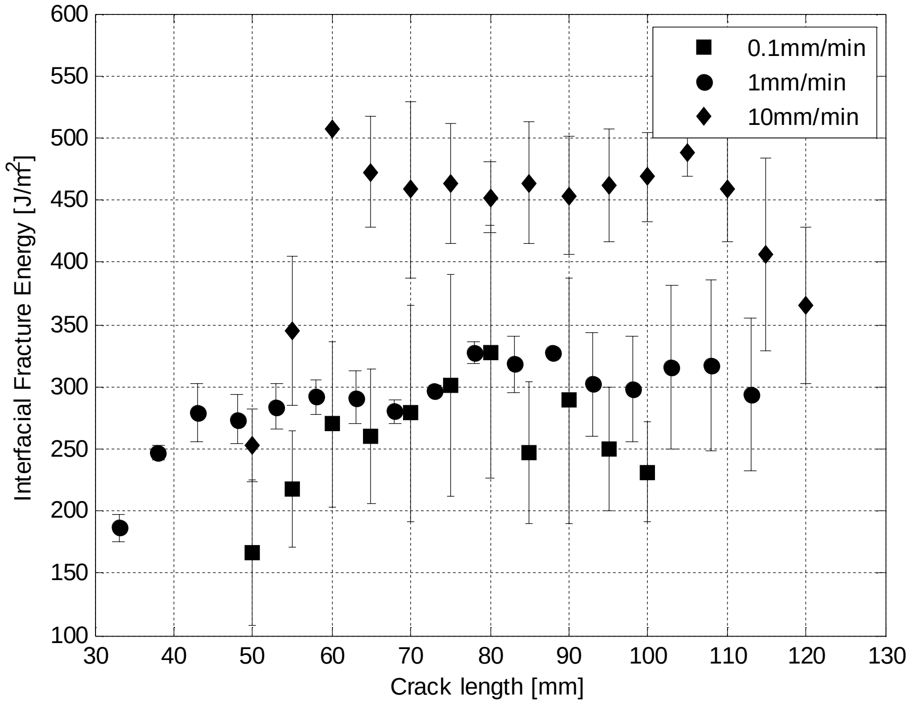

Fig. 7. The interfacial fracture energy of composite/rubber interface for three different loading rates. Rubber thickness was 0.7 mm.

Table 1. The average value and the standard deviation of the maximum load for the different sample types.

Sample	F_{max} [N]	STDEV [N]
0.5 mm @ 1 mm/min	*100.5*	*7.6*
0.7 mm @ 1 mm/min	*90.6*	*2.1*
0.7 mm @ 0.1 mm/min	*64.3*	*2.3*
0.7 mm @ 10 mm/min	*87.2*	*3.4*

Table 2. The average *m* and C_0 values (Equations 1 and 2) for the different sample types.

Sample	*m* [1/kN mm^2]	C_0 [mm/kN]
0.5 mm @ 1 mm/min	0.0003	21.5
0.7 mm @ 1 mm/min	0.0003	22.1
0.7 mm @ 0.1 mm/min	0.0002	33.7
0.7 mm @ 10 mm/min	0.0002	27.6

Table 3. Average interfacial fracture energies $G_{I/IIC}$ for different sample types.

Sample	$G_{I/IIC}$ [J/m^2]
0.5 mm @ 1 mm/min	353
0.7 mm @ 1 mm/min	290
0.7 mm @ 0.1 mm/min	258
0.7 mm @ 10 mm/min	435